ЖУРНАЛ СТРУКТУРНОЙ ХИМИИ

2015. Том 56, № 4 *Июль* *С. 773 – 779*

UDC 548.73:547.13:546.73

A NEW 2D COBALT(II) COORDINATION POLYMER CONSTRUCTED FROM 1,2,4,5-BENZENETETRACARBOXYLATE AND FLEXIBLE BIS(BENZIMIDAZOLE) LIGANDS

X. Du, R. Yang, X.X. Wang, G.H. Cui

College of Chemical Engineering, Hebei United University, Tangshan, Hebei Province, P. R. China
E-mail: tscghua@126.com

Received September 16, 2013

A new 2D cobalt(II) coordination polymers namely $\{[Co_2(btec)(L)_2]\cdot 4H_2O\}_n$ (**1**), where btec = = 1,2,4,5-benzenetetracarboxylate and L = 1,3-bis(5,6-dimethylbenzimidazol-l-yl)-2-propanol, are hydrothermally synthesized and characterized by elemental analyses, IR spectroscopy, and single crystal X-ray diffraction analyses. The structure analysis indicates that the compound belongs to the triclinic system, space group $P\bar{1}$, $a = 12.198(2)$ Å, $b = 15.0750(2)$ Å, $c = 15.194(2)$ Å, $\alpha = 77.420(2)°$, $\beta = 77.872(2)°$, $\gamma = 85.538(2)°$, $V = 2664.2(5)$ Å^3, $Z = 2$. The complex possesses a binodal (3,4)-connected two-dimensional layered structure bridged by btec and L ligands. The fluorescence and catalytic properties of the complex are also investigated.

DOI: 10.15372/JSC20150416

K e y w o r d s: 1,2,4,5-benzenetetracarboxylate, bis(benzimidazole), cobalt(II), fluorescence property.

INTRODUCTION

The rational design and synthesis of MOFs have attracted intense attention, which is propelled by their potential applications as functional materials in adsorption, separation, magnetism, luminescence, catalysis and so on [1—6]. In the past decades, considerable progress has been achieved in controlling the assembly and orientations of individual molecules in structures with specific network topologies and potentially interesting properties. It is well known that the coordination geometries of the metal centers and the coordination behavior of organic ligands are the main keys to achieve the target coordination polymers. Benzene-based multicarboxylic acid ligands have been widely used as good candidates for the construction of coordination polymers [7—9]. For example, 1,2,4,5-benzene tetracarboxylate (btec) has various coordination modes to metal ions, resulting from completely or partially deprotonated sites, which allows for the diversity of framework topologies of MOFs. On the other hand, the most prominent compound of benzimidazole derivatives is 5,6-dimethylbenzimidazole, which serves as an axial ligand for cobalt in vitamin B_{12} [10—13]. To the best of our knowledge, coordination polymers based on flexible bis(5,6-dimethybenzimidazole) and multicarboxylic acid ligands have only been scarcely studied [14—16]. In this report, we focus our continuing efforts on coordination polymers based on flexible bis(5,6-dimethybenzimidazole) ligands [17—20]; here we report the preparation, crystal structure, and fluorescence properties of a new two-dimensional framework $\{[Co_2(btec)(L)_2]\cdot 4H_2O\}_n$ (**1**) L = 1,3-bis(5,6-dimethylbenzimidazol-l-yl)-2-propanol). The effective degradation of methyl orange (MO) used as a catalyst is also investigated.

© Du X., Yang R., Wang X.X., Cui G.H., 2015

EXPERIMENTAL

Reagents and apparatus. All the solvents and reagents for the synthesis were purchased from Sigma—Aldrich unless otherwise specified and used as received. The ligand L was prepared according to the literature method with a minor modification [21]. Elemental analyses were taken on a Perkin-Elmer 240C analyzer. IR spectra (KBr pellet) were obtained on a FT-IR 170 SX (Nicolet) spectrometer. Fluorescence spectra were measured on a Hitachi F-7000 fluorescence spectrophotometer at room temperature.

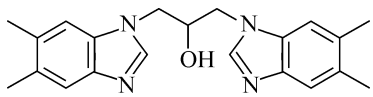

Scheme 1

X-Ray crystallography. The single crystal X-ray diffraction measurement was carried out on a Bruker Smart 1000 CCD diffractometer equipped with a graphite crystal monochromator situated in the incident beam for data collection at 293(2) K. Reflection intensities were measured using graphite-monochromatized MoK_α radiation ($\lambda = 0.71073$ Å) with the ω scan mode in the range $1.38 < \theta < 27.49°$. Unit cell dimensions were obtained with least-squares refinements and semi-empirical absorption corrections were applied using the SADABS program [22]. The structure was solved by a direct method [23] and non-hydrogen atoms were obtained in successive difference Fourier syntheses. The final refinements were performed by full-matrix least-squares methods on F^2 using the SHELXL-97 program package [24]. The summary of the crystallographic data and structure analysis is given in Table 1, and the selected bond lengths and angles are listed in Table 2. CCDC 961062 contains the

Table 1

Crystal data and structure refinement for **1**

Empirical formula	$C_{52}H_{57}Co_2N_8O_{14}$
CCDC number	
Formula weight	1135.92
Temperature, K	293(2)
Wavelength, Å	0.71073
Crystal system	Triclinic
Space group	$P\bar{1}$
Unit cell dimensions a, b, c, Å	12.198(2), 15.0750(2), 15.194(2)
α, β, γ, deg.	77.420(2), 77.872(2), 85.538(2)
Volume, Å^3	2664.2(5)
Z	2
d_{calc}, g/cm^3	1.416
μ, mm^{-1}	0.696
F(000)	1182
Crystal size, mm	0.13×0.11×0.10
θ range, deg.	1.38 to 27.49
Range of h, k, l	–15/14, –17/19, –16/19
Reflections collected / unique	16412 / 11794
Max. and min. transmission	0.928 and 0.854
Refinement method	Full-matrix least-squares on F^2
Data / restraints / parameters	11794 / 0 / 706
Goodness-of-fit on F^2	0.896
Final R indices [$I > 2\sigma(I)$]	$R1 = 0.0851$, $wR2 = 0.2418$
R indices (all data)	$R1 = 0.1652$, $wR2 = 0.3111$
Residual peak and hole, e/Å^3	1.602 and –0.570

Table 2

Selected bond lengths (Å) *and angles* (deg.) *for complex* **1**

Co1—O2	1.953(4)	O2—Co1—O7	107.12(19)	O2—Co1—N7	126.5(2)
Co1—N7	2.033(5)	O7—Co1—N7	111.1(2)	O2—Co1—N5	100.4(2)
Co2—O3	1.938(4)	O7—Co1—N5	109.7(2)	N7—Co1—N5	100.4(2)
Co2—N1	2.022(6)	O3—Co2—O5	112.9(2)	O3—Co2—N1	99.7(2)
Co1—O7	1.974(4)	O5—Co2—N1	108.1(2)	O3—Co2—N3	108.7(2)
Co1—N5	2.046(6)	O5—Co2—N3	118.2(2)	N1—Co2—N3	107.4(2)
Co2—O5	1.960(4)	C22—O5—Co2	110.9(4)	C31—O7—Co1	106.5(4)
Co2—N3	2.031(6)	C23—O3—Co2	126.4(4)	C32—N7—Co1	125.5(5)
		C33—N7—Co1	129.6(4)	C1—N1—Co2	125.7(5)
		C2—N1—Co2	130.0(5)	C13—N3—Co2	126.2(5)
		C21—N3—Co2	130.3(4)	C44—N5—Co1	123.7(5)
		C45—N5—Co1	131.8(5)		

Symmetry code: #1 = $-x+2$, $-y+1$, $-z+2$, #2 = $-x+2$, $-y+2$, $-z+1$, #3 = $x-1$, y, $z+1$, #4 = $x+1$, y, $z-1$.

supplementary crystallographic data for the complex. These data can be obtained from the Cambridge Crystallographic Data Centre, 12 Union Road, Cambridge CB2 1EZ, UK; Fax: +44-1223-336033; E-mail: deposit@ccdc.cam.ac.uk.

Catalytic experiments. The catalytic performance of the complex was investigated with degradation of methyl orange through a typical process: 50 mg of the title compounds and 30 mg of sodium persulfate were mixed together with 150 ml of the methyl orange solution (10 mg/l). The experiments were performed at 30 °C, and the pH was adjusted to 3.0 by the dropwise addition of 0.1 mol/l H_2SO_4 as required. Samples of the mixture were withdrawn and analyzed periodically using a SHANGHAI JINGKE 722 N spectrophotometer at 506 nm. This procedure was also carried out in the absence of the catalyst as a control experiment under the same conditions. The degradation efficiency of methyl orange is defined as follows:

$$\text{Degradation efficiency} = 100\ \% \times (1 - C_t/C_0), \quad (1)$$

where C_0 (mg/l) is the initial concentration of methyl orange and C_t (mg/l) is the concentration of methyl orange at the reaction time t (min).

Synthesis of $\{[Co_2(btec)(L)_2]\cdot 4H_2O\}_n$ (1). A mixture of cobalt(II) chloride (0.3 mmol, 71 mg), the L ligand (0.1 mmol, 35 mg), 1,2,4,5-benzenetetracarboxylic acid (H_4btec, 0.10 mmol, 25.4 mg), H_2O (15 ml), and NaOH (0.4 mmol, 1.6 mg) were placed in a Teflon-lined stainless vessel and heated to 140 °C for 4 days under autogenous pressure, and then cooled to room temperature at a rate of 10 °C/h. The crystals of the complex were obtained in a 36.7 % yield based on Co. Anal. calcd. for $C_{52}H_{57}Co_2N_8O_{14}$ (%): C, 54.93; H, 5.02; N, 9.86. Found (%): C, 54.79; H, 5.08 N, 9.69. IR (KBr pellet, cm^{-1}): 3428(s), 1624(m), 1512(s), 1392(m), 1080(m), 960(w), 698(w), 466(m).

RESULTS AND DISCUSSION

Syntheses and general methods. The reaction of $CoCl_2$, 1,2,4,5-benzenetetracarboxylate, and the ligand L in the aqueous system gave rise to a coordination polymer under the hydrothermal condition. The results of the elemental analyses for the complex were in good agreement with the theoretical requirements of their compositions (X-ray analysis results). IR spectra of the compound show strong absorption around 1512 cm^{-1}, which can be assigned to the $\nu_{C=N}$ stretching vibration of the benzimidazole ring of the L ligand. No strong absorption peaks are observed around 1700 cm^{-1} for carboxylate groups, indicating that all carboxylic groups are deprotonated in the complex. The antisymmetric and

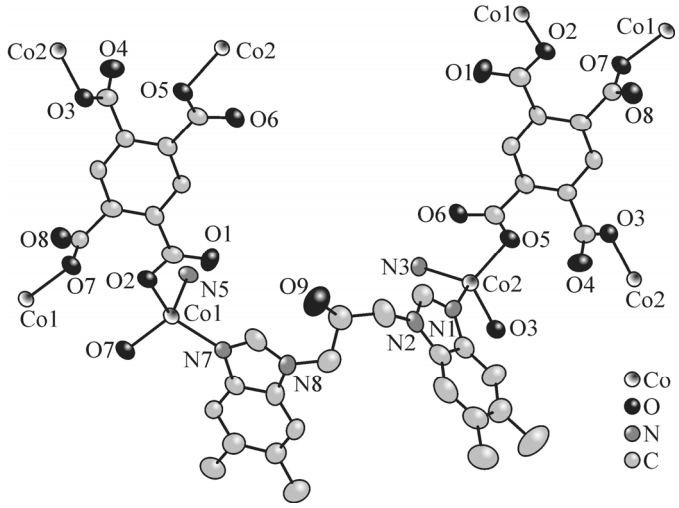

Fig. 1. Metal coordination environment in the complex with the labelling scheme and 30 % thermal ellipsoids. Hydrogen atoms are omitted for clarity. (Symmetry code: #1 = $-x+2, -y+1, -z+2$, #2 = $-x+2, -y+2, -z+1$, #3 = $x-1, y, z+1$, #4 = $x+1, y, z-1$)

symmetric vibrations of the carboxylate groups appear at 1624 cm^{-1} and 1392 cm^{-1} for the compound. The $\Delta\nu$ values, which represent the separation between $\nu_{asym}(CO_2)$ and $\nu_{sym}(CO_2)$, are 232 cm^{-1}, which confirms that the carboxylic groups are monodentate in both complexes.

Description of the crystal structure. The single crystal X-ray diffraction analysis shows that the complex crystallizes in the triclinic $P\bar{1}$ space group. The asymmetric unit of the complex contains two Co^{2+} ions, two μ_2-L ligands, one fully-deprotonated $btec^{4-}$ anion, and four lattice water molecules. As shown in Fig. 1, the coordination environment around Co1, Co2 atoms is best portrayed as a distorted tetrahedral geometry with τ_4 factors of 0.87 and 0.91 respectively [25]. Both Co atoms are surrounded by N atoms from two different L ligands and two O atoms from distinct monodentate carboxylic groups of $btec^{4-}$. The Co—O and Co—N bond lengths vary from 1.938(4) Å to 1.974(4) Å and from 2.022(6) Å to 2.046(6) Å, respectively. They are comparable to those of similar cobalt complexes.

The rigid carboxyl groups of $btec^{4-}$ ligands are fully deprotonated and take the monodentate coordination mode. Each $btec^{4-}$ ligand bridges the neighboring Co^{2+} ions to form a one-dimensional ladder-like chain $[Co_2(btec)]_n$, obviously including a binuclear unit, with the distances Co1···Co1 = = 5.2976(1) Å and Co2···Co2 = 5.341(1) Å respectively. The intrachain Co1···Co2 distances are 8.743(1) Å and 10.252(2) Å. These chains are further extended by μ_2-L ligands to build a two-dimensional $[Co_2(btec)(L)_2]_n$ layer (Fig. 2), the Co···Co distance between two adjacent chains being 10.163(2) Å. The two μ_2-L ligands connect two Co atoms as a bridge, with the dihedral angles of the two adjacent benzimidazole rings being 82.207(3) Å and 86.857(3) Å.

There are two modes of π—π stacking interactions between two benzimidazole rings of L with center-to-center distances of 3.730(4) Å and 3.545(4) Å in the complex, which can further stabilize the crystal packing.

The polycarboxylic $btec^{4-}$ ligand and the metal unit are both viewed as a node in the process of the topological analysis. If the $btec^{4-}$ ligands are considered as a four-connected node, the Co^{2+} ions are viewed as a three-connected node, and the L ligand acts as linker, then it presents a novel binodal(3,4)-connected network with a point symbol of $\{4.6^2\}_2\{4^2.6.^2.8^2\}$, simplified and analyzed by TOPOS4.0 [26] (Fig. 3).

Powder X-ray diffraction (XRD). The complex was characterized by powder XRD at room temperature (Fig. 4). It is clear that in the experimental patterns the peak positions are well matched to the corresponding simulated patterns generated by the Mercury Program [27] using the single crystal

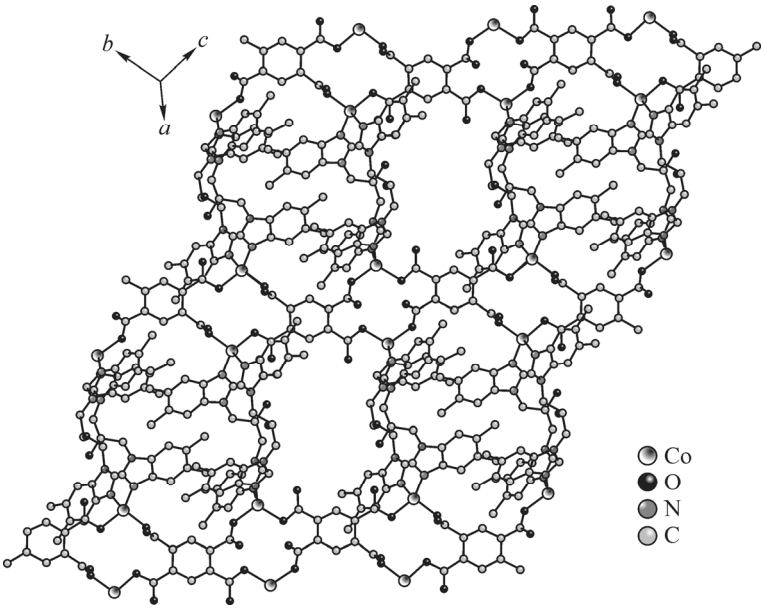

Fig. 2. 2D layer of the complex

X-ray diffraction data, thus confirming the phase purities of the complex. The differences in peak intensities for the simulations may be due to the preferred orientation of the powder samples.

Fluorescence of the complex. The luminescent behavior of the coordination polymer and the free L ligand was studied in the solid state at room temperature; emission spectra are shown in Fig. 5. The free L ligand displays luminescence with an emission band at 445 nm (under 390 nm excitation). Meanwhile, the emission for the complex can be observed, where the emission bands appear at 369 nm (under 335 nm excitation). In comparison to that of the free ligand, a blue shift of ca. 76 nm is strong in complex, which may be due to an increase in the conjugation upon the metal coordination and originate from the ligand-to-metal charge-transfer (LMCT) [28].

Catalytic degradation of methyl orange. A new advanced oxidation technology based on strongly oxidizing sulfate radicals ($SO_4^{\bullet -}$) has recently been developed to degrade recalcitrant organic pollutants [29]. As Fenton′s reagent, persulfate anions can produce sulfate radicals; however, the un-

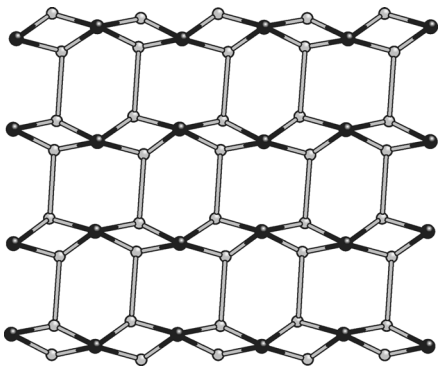

Fig. 3. (3,4)-connected topological network of the complex

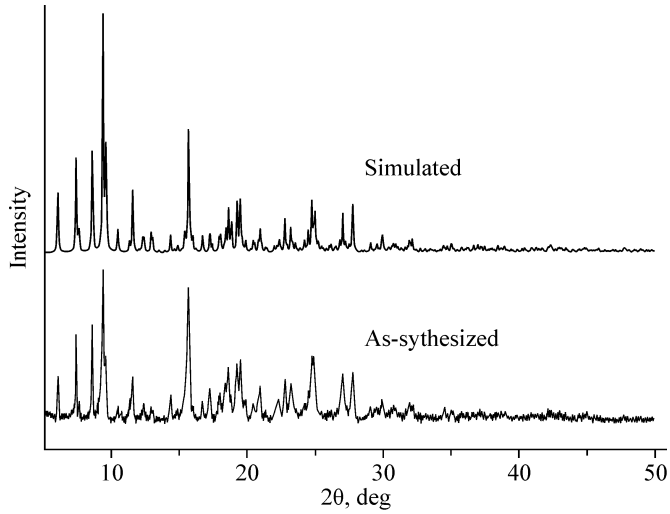

Fig. 4. Powder XRD pattern of the complex

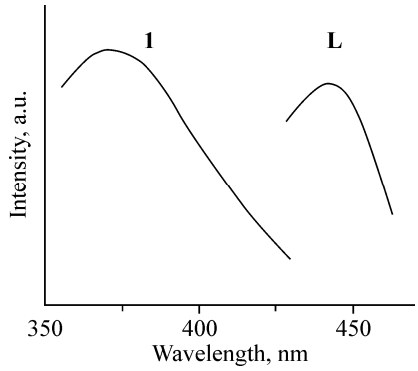

Fig. 5. Solid-state fluorescence spectra of L and the complex

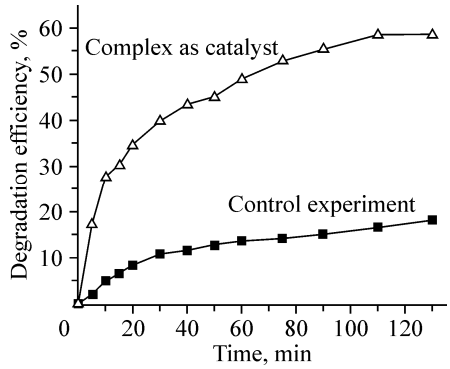

Fig. 6. Experimental results of the methyl orange degradation

catalyzed reaction rate is extremely slow. We used the cobalt(II) coordination polymers as heterogeneous catalysts to activate persulfate anions and generate sulfate radicals ($SO_4^{\bullet -}$). It is possible to represent the mechanism according to Equations (2)—(4) respectively [30].

$$\text{MOF—Co}^{2+} + S_2O_8^{2-} \rightarrow \text{MOF—Co}^{3+} + SO_4^{2-} + SO_4^{\bullet -}, \quad (2)$$

$$\text{MoF—Co}^{3+} + S_2O_8^{2-} \rightarrow \text{MOF—Co}^{2+} + 2SO_4^{\bullet -}, \quad (3)$$

$$\text{Azo dye} + SO_4^{\bullet -} \rightarrow \text{oxidation products}. \quad (4)$$

The methyl orange degradation experiments were carried out and the results are depicted in Fig. 6 (the vertical axis shows the degradation efficiency of methyl orange at the time *t*). It is obvious that the complex has a higher activity on catalyzing the degradation of methyl orange. The catalytic activity of the complex is stable and can be maintained under ambient conditions, but more important is that the degradation efficiency has values up to 61.84 % under the optimal conditions of 130 min; whereas when the control experiments were carried out, the degradation efficiency reduced to 21.07 % in 130 min.

REFERENCES

1. *Deng H., Doonan C.J., Furukawa H.* // Science. – 2010. – **327**. – P. 846 – 850.
2. *Zhang J., Wojtas L., Larsen R.W.* // J. Am. Chem. Soc. – 2009. – **131**. – P. 17040 – 17041.
3. *O'Keeffe M., Peskov M.A., Ramsden S.J.* // Acc. Chem. Res. – 2008. – **41**. – P. 1782 – 1789.
4. *Pramanik S., Zheng C., Emge T.J.* // J. Am. Chem. Soc. – 2011. – **133**. – P. 4153 – 4155.
5. *Geng J.C., Qin L., Du X.* // Z. Anorg. Allg. Chem. – 2012. – **638**. – P. 1233 – 1238.
6. *Li H., Davis C.E., Groy T.L.* // J. Am. Chem. Soc. – 1998. – **120**. – P. 2186 – 2187.
7. *Geng J.C., Cui G.H., Jiao C.H.* // J. Chin. Chem. Soc. – 2012. – **59**. – P. 704 – 709.
8. *Ma L.F., Qin J.H., Wang L.Y.* // RSC Advances. – 2011. – **1**. – P. 180 – 183.
9. *Gandolfo C.M., LaDuca R.L.* // Cryst. Growth Des. – 2011. – **11**. – P. 1328 – 1337.
10. *Geng J.C., Qin L., He C.H.* // Transition Met. Chem. – 2012. – **37**. – P. 579 – 585.
11. *Cui G.H., He C.H., Jiao C.H.* // CrystEngComm. – 2012. – **14**. – P. 4210 – 4216.
12. *Jiao C.H., Geng J.C., He C.H.* // J. Mol. Struct. – 2012. – **1020**. – P. 134 – 141.
13. *Jiao C.H., He C.H., Geng J.C.* // J. Coord. Chem. – 2012. – **65**. – P. 2852 – 2861.
14. *Zheng S.T., Zhang J., Li X.X.* // J. Am. Chem. Soc. – 2010. – **132**. – P. 15102 – 15103.
15. *Horike S., Bureekaew S., Kitagawa S.* // Chem. Commun. – 2008. – P. 471 – 473.
16. *Wang X.L., Yang S., Liu G.C.* // Inorg. Chim. Acta. – 2011. – **375**. – P. 70 – 76.
17. *Yang E.C., Liu Z.Y., Shi X.J.* // Inorg. Chem. – 2010. – **49**. – P. 7969 – 7975.
18. *Liu Q.X., Zhao Z.X., Zhao X.J.* // Cryst. Growth Des. – 2011. – **11**. – P. 4933 – 4942.
19. *Liu T.F., Wu W.F., Zhang W.G.* // Anorg. Allg. Chem. – 2011. – **637**. – P. 148 – 153.
20. *Cui G.H., Li J.R., Hu T.L.* // J. Mol. Struct. – 2005. – **738**. – P. 183 – 187.
21. *Chang Q., Meng X.R., Song Y.L., Hou H.W.* // Chinese J. Chem. – 2005. – **23**. – P. 725.

22. *Sheldrick G.M.* SADABS, Program for Empirical Absorption Correction of Area Detector Data, Univ. Göttingen, Germany, 1996.
23. *Sheldrick G.M.* SHELXLS-97, Program for X-ray Crytal Structure Solution, Univ. Göttingen, Germany, 1997.
24. *Sheldrick G.M.* SHELXL-97, Program for X-ray Crystal Structure Refinement, Univ. Göttingen, Germany, 1997.
25. *Yang L., Powell D.R., Houser R.P.* // Dalton Trans. – 2007. – **9**. – P. 955 – 964.
26. *Blatov V.A.* // Struct. Chem. – 2012. – **23**. – P. 955 – 963; http: // www.topos.samsu.ru.
27. *Macrae C.F., Edgington P.R., McCabe P.* // J. Appl. Crystallogr. – 2006. – **39**. – P. 453 – 457.
28. *Cui Y., Yue Y., Qian G., Chen B.* // Chem. Rev. – 2012. – **112**. – P. 1126 – 1162.
29. *Ocampo M.* Persulfate Activation by Organic Compounds, Thesis for the Doctorate, Washington State University, 2009.
30. *Liu J.M., Lin X., Wei C.J.* // Microchim. Acta. – 2004. – **148**. – P. 267 – 272.